

Journal of Materials Chemistry B

Accepted Manuscript



This is an *Accepted Manuscript*, which has been through the Royal Society of Chemistry peer review process and has been accepted for publication.

Accepted Manuscripts are published online shortly after acceptance, before technical editing, formatting and proof reading. Using this free service, authors can make their results available to the community, in citable form, before we publish the edited article. We will replace this *Accepted Manuscript* with the edited and formatted *Advance Article* as soon as it is available.

You can find more information about *Accepted Manuscripts* in the [Information for Authors](#).

Please note that technical editing may introduce minor changes to the text and/or graphics, which may alter content. The journal's standard [Terms & Conditions](#) and the [Ethical guidelines](#) still apply. In no event shall the Royal Society of Chemistry be held responsible for any errors or omissions in this *Accepted Manuscript* or any consequences arising from the use of any information it contains.

Surface Modification of Titanium with Curcumin: A Promising Strategy to Combat Fibrous Encapsulation

Cite this: DOI: 10.1039/x0xx00000x

Received 00th January 2012,
Accepted 00th January 2012

DOI: 10.1039/x0xx00000x

www.rsc.org/

Ronghan He,^{a,b} Xuefeng Hu,^a Hark Chuan Tan,^a Jason Feng,^c Chris Steffi,^a Kun Wang,^b and Wilson Wang^a

Fibrous encapsulation that prevents the direct contact between an implant and the bone can cause implant failure. However, prevention of fibrous encapsulation is difficult due to the lack of effective strategies which can selectively control the growth of fibroblasts and osteoblasts. Since curcumin, an extract from *Curcuma longa*, was recently found to reduce the formation of fibrous tissue, we hypothesize that loading curcumin on implant surfaces would be efficacious to inhibit fibrous encapsulation without adversely affecting osteoblast functions. To prove this hypothesis, curcumin was loaded on titanium surface by using polydopamine as an anchor, and the behaviors of fibroblasts and osteoblasts on these curcumin-modified surfaces were investigated. Curcumin was successfully loaded on titanium with low release after incubation in phosphate-buffered saline (PBS) for 7 days. On the curcumin-modified surfaces, fibroblast proliferation was suppressed, and fibrous marker expressions as well as collagen synthesis were significantly reduced. These reductions were possibly due to the enhancement of fibroblast apoptosis induced by the surface curcumin. In contrast, no significant reduction in osteoblast functions was observed on the curcumin-modified substrates. These findings may provide a promising solution to reduce fibrous encapsulation, and thus may be highly beneficial for orthopaedic applications.

Introduction

Nowadays, arthroplasty has been developed into a gold standard for the treatment of disabling osteoarthritis. However, approximately 10% of these metal implants used in the surgeries will fail because of loosening, and the required surgical revision of the failed implants brings a considerable burden to the society and patients.^{1,2} Fibrous encapsulation is detrimental to implant fixation, which is a strong contributor to later failure of the implants.³ Usually for most of the failed implants, large amount of fibrous encapsulation can be found on implant-bone interfaces, which prevents effective osseointegration (i.e. the direct contact between bone and the implant) and causes implant loosening.⁴⁻⁶ In addition, the formed fibrous tissue can also increase intraarticular pressure, resulting in the extension of the gap between bone and the implant and subsequently implant loosening.^{7,8}

Although fibrous encapsulation can induce implant loosening, it receives insufficient scientific and clinical attention. Hardly any appropriate strategies have been developed or proposed for prevention of fibrous encapsulation

on implant surfaces.⁵ Many factors may regulate the formation of fibrous encapsulation around the implant, such as particulate wear debris and implant micromotion on implant-bone interfaces.³ Under controlled conditions where these factors have been eliminated, fibroblasts are the key cellular factors for the formation of fibrous tissue, the reduction of fibrous encapsulation can be achieved via inhibiting the growth of fibroblasts on implant surfaces.⁹ In addition, inhibition of fibroblast growth may also help to enhance bone formation since fibroblasts can produce cytokines that can activate osteoclast activities and suppress osteoblast functions.^{10,11}

Surface modification is an effective method to regulate the behavior of cells on implant surfaces. Thus, selectively control of cell growth on implant surfaces can be achieved via proper surface modification.¹² However, it is difficult to inhibit fibroblast growth on implant surfaces by using a single or several cytokines due to the great heterogeneity of fibroblasts and the capability to receive stimuli from different cells.^{13,14} In addition, the technique developed for the inhibition of fibroblast growth should not exhibit adverse effects on

osteoblast functions, because osteoblasts are the cells for new bone formation.¹⁵ Previous *in vitro* works from our group demonstrate that metal surfaces modified with bone morphogenic protein-7 (BMP-7) peptide¹⁶ and alendronate¹⁷ can inhibit fibroblast growth. However, these two agents used have been reported to have adverse side effects on bone metabolism, such as ectopic calcification (stimulated by BMP-7 peptide¹⁸) and osteonecrosis of the jaws (ONJ) (induced by alendronate¹⁹), which could limit the applications of those modified implants.

Curcumin, a natural polyphenolic compound derived from *Curcuma longa*, possesses anti-inflammatory, potent anti-oxidant and anti-carcinoma effects,²⁰⁻²² and has been used as an alternative of drugs for a wide range of conditions such as colon cancer, arthritis and Alzheimer's disease.²³ Particularly, curcumin can prevent the formation of fibrotic tissues in lung, kidney and liver fibrosis.²⁴⁻²⁷ At tissue level, administration of curcumin results in a significant reduction of fibrous tissue.²⁸ At cellular level, it has been reported that curcumin can significantly inhibit the migration and proliferation of fibroblasts.²⁹ In addition, curcumin has been proven to exhibit no deleterious side effect in the human body even with the doses of 2-12 g/day.³⁰ The characters of curcumin may be beneficial for orthopaedic applications to prevent fibrous encapsulation on implant surfaces.

Thus, we hypothesize that modification of implant surface with curcumin would be a solution to combat fibrous encapsulation in orthopaedics without adversely affecting osseointegration. To verify this hypothesis, curcumin was immobilized on the surface of Ti with polydopamine as an anchor, and the behaviors of fibroblasts on the modified surfaces were investigated. The investigations on the effects of the immobilized curcumin on osteoblasts were also conducted to investigate the potential applications in orthopedics.

Materials and Methods

Materials

Ti sheets were purchased from Goodfellow Cambridge Ltd (Huntingdon, UK). Mouse fibroblasts (NIH3T3, CRL-1658) and osteoblasts (MC3T3-E1 subclone 14) were obtained from American Type Culture Collection (Manassas, VA). Curcumin [1,7-bis(4-hydroxy-3-methoxy-phenyl)-1,6-hexadiene-3,5-dione], pepsin, dopamine hydrochloride, 2-hydroxypropyl- β -cyclodextrin (HP- β -CD), and alizarin red were obtained from Sigma-Aldrich (St. Louis, USA). Primers for quantitative reverse transcriptase polymerase chain reaction (qRT-PCR) were commercially synthesized by 1st BASE Pte Ltd (Singapore).

Substrate preparation

Ti sheets were cut into $1 \times 1 \text{ cm}^2$ dimensions, then cleaned ultrasonically for 15 min in Kroll's reagent (7.2% HNO_3 , 4.0% HF, 88.8% water).³¹ The substrates were then rinsed thoroughly with distilled water. Polydopamine was first coated on Ti

(termed as the Ti-PDOP substrate) via immersion of the washed Ti substrates in a dopamine solution (2 mg/mL in 10 mM Tris buffer, pH 8.5) overnight in the dark,¹⁶ followed by washing with distilled water to remove the unreacted dopamine and drying under nitrogen flow. Each Ti-PDOP substrate was then immersed in 0.1 mL of curcumin loading solutions (10 μM and 20 μM in distilled water) for 24 h at room temperature followed by triple washing with distilled water and drying in a stream of nitrogen. The prepared substrates were termed as Ti-PDOP-curcumin10 and Ti-PDOP-curcumin20, respectively.

Characterization

The chemical compositions of the surfaces were characterized by X-ray photoelectron spectroscopy (XPS) on a Kratos AXIS Ultra^{DLD} spectrometer (Kratos Analytical, UK) with an Al $K\alpha$ X-ray source (1486.7 eV photons).³² All binding energies (BEs) were referenced to the C 1s (C-C bond) peak at 284.6 eV. The immobilized curcumin was directly observed by using HP- β -CD since HP- β -CD can bind to curcumin and significantly enhance the fluorescence from curcumin.^{32,33} In brief, each substrate was immersed in 0.2 mL of 1% methanol aqueous solution containing 30 mM of HP- β -CD for 30 min followed by washing twice with methanol,³⁴ and then observed with a confocal laser scanning microscope (CLSM, Olympus, Japan). To determine the surface density of immobilized curcumin on the substrates, the loading solution after curcumin immobilization was combined with the washing solution, and the curcumin concentration in the combined solution was determined using the high performance liquid chromatography (HPLC) system (HPLC 1200 system, Agilent, USA) on a Venusil XBP-C18 column with detection at 425 nm. A solution of 50% acetonitrile in 2% acetic acid in water was used as the mobile phase, and the flow rate was 1.0 mL/min.³⁵ A standard curve was obtained by analyzing curcumin solutions of known concentrations. The surface density of immobilized curcumin was determined by the difference between the amount of curcumin in the initial loading solution and that remaining in the combined solution.

Curcumin release assay

Tests to analyze the possible release of curcumin from the substrates were performed via immersion of each substrate in 1 mL of phosphate-buffered saline (PBS) over 10 days. The substrates were immersed in PBS for different periods (3, 6, 12, 24, 48, 72, 120, 168 and 240 h). After that, the amount of curcumin released in the PBS was tested with HPLC as described above.

Cell culture

Fibroblasts were cultured in a growth medium of Dulbecco's modified Eagle's medium (Invitrogen, USA) supplemented with 10% fetal calf serum (HyClone, USA), 100 unit/mL penicillin, and 100 mg/mL streptomycin (Invitrogen, USA). Osteoblasts were cultured in a growth medium of Alpha Minimum Essential Medium (Invitrogen, USA) with 10% fetal bovine serum, 100 unit/mL penicillin, and 100 mg/mL

streptomycin. Cells were grown at 37 °C under a moist atmosphere of 5% CO₂ in air. The medium was changed every couple of days.

Cell attachment and proliferation assay

Substrates of Ti, Ti-PDOP, Ti-PDOP-curcumin10 and Ti-PDOP-curcumin20 were used for cell attachment and proliferation assay. Each substrate was placed in one well of a 24-well microplate. For cell attachment assay, 100 µL of cell suspension containing 30,000 cells was seeded carefully on each substrate to avoid cell adhesion on the well. After incubation for 6 h at 37 °C, all the substrates were carefully rinsed thrice with PBS to remove the unattached cells. The adherent cells were then detached by trypsin and counted with a Scepter coulter-method-based automated cell counter (Millipore, USA). For the proliferation assay, cells were seeded on each substrate at a density of 10,000 cells/cm². After 1, 3, and 7 days of culture, the number of cells on the substrate was counted as described above and cell metabolic activity was tested by thiazolyl blue tetrazolium bromide (MTT) assay.³⁶

Fibroblast and osteoblast apoptosis assays

Fibroblasts or osteoblasts were seeded on each substrate at a density of 30,000 cells/cm². After 48 h of culture, the medium was removed and the cells on the substrates were washed with ice-cold PBS. To investigate the apoptosis of fibroblasts on the substrates, the cells were then trypsinized from the substrates and stained with a FITC Annexin V/Dead Cell Apoptosis Kit (Invitrogen, USA) according to the manufacturer's instructions.³⁷ The stained cells were analyzed by a flow cytometer (CyAnTM ADP analyser, Beckman Coulter). To obtain a positive control, fibroblasts were seeded on pristine Ti and cultured for 2 days. After that, the cells on Ti were treated with 10 µM camptothecin (Sigma-Aldrich, USA) supplemented in growth medium for 4 h in 37 °C (to induce cell apoptosis), and then trypsinized and stained for the flow cytometry analysis as described above. Data were analyzed after the adjustment of color compensation for each individual color. Apoptotic fibroblasts were also observed by fluorescence microscopy. Briefly, after the cells were trypsinized, resuspended and stained with the FITC Annexin V/Dead Cell Apoptosis Kit (as described above), they were fixed onto slides with 4% paraformaldehyde (PFA) in PBS for 15 min. A cover slip was then mounted on the slide with mounting medium containing DAPI (Fluoroshield, Sigma-Aldrich), and the cells were examined under a Nikon Eclipse Ti inverted microscope system with C-HGFIE Intensilight fiber illuminator.

Collagen assay and collagen type I staining

Fibroblasts were seeded on each substrate at a density of 30,000 cells/cm², and then cultured in growth medium supplemented with 50 µM of ascorbic acid (Wako, Japan) for 7 and 14 days. After removal of the medium, the extracellular collagen produced by fibroblasts was extracted via incubation of each substrate in 1 mL of pepsin solution (0.1 mg/mL in 0.5 M acetic acid) overnight at 4 °C. The extracted collagen was quantified

utilizing a SircolTM Collagen Assay Kit (Biocolor, UK) as per the manufacturer's instructions.³⁸ The collagen produced by fibroblasts on each substrate was also qualitatively imaged after staining with a collagen type I antibody.³⁹ Briefly, fibroblasts on each substrate were fixed by 4% PFA for 15 min, and then permeabilized with 0.1% Triton X-100 solution followed by incubation in 1 mL of 2% bovine serum albumin (BSA) at room temperature for 2 h. The substrates were then incubated with 5 µg/mL rabbit anti-mouse collagen type I primary antibody (Millipore, USA) at room temperature for 2 h, followed by incubation with a secondary antibody, Alexa Fluor 488 goat anti-mouse IgG (Life Technologies, USA) for 1 h. After the collagen staining process, the cells on the substrates were stained with DAPI (Fluoroshield, Sigma-Aldrich), and then visualized using CLSM.

Quantitative reverse transcriptase polymerase chain reaction (qRT-PCR)

The gene expressions of fibrous markers were characterized by using qRT-PCR as described in a previous work from our group.¹⁶ Fibroblasts were seeded on each substrate at a density of 30,000 cells/cm², and then cultured for one or two weeks. mRNA extractions were conducted by using a RNeasy Kit with QIAshredder (QIAGEN, Netherlands) as per the manufacturer's instructions. mRNA concentrations were analyzed with a Nanodrop 1000 spectrophotometer (ThermoScientific, USA). 10 ng of the synthesized mRNA was used for cDNA synthesis with a Superscript Vilo cDNA Synthesis Kit (Invitrogen, USA) on an iCycler thermal cycler (Bio-Rad, USA). qRT-PCR was then performed using an Express GreenER QPCR AB Kit (Invitrogen, USA) on a StepOneTM Plus real-time PCR system (Applied Biosystems) according to the manufacturer's instructions. The amplification specificity was assessed based on dissociation curves. The relative expressions of the target genes were normalized to the reference gene *Gapdh*. The sequences of the primers used are summarized in Table S1.

Alkaline phosphatase activity assay

The alkaline phosphatase (ALP) was performed according to the procedure described in a previous work from our group.¹⁷ Osteoblasts were seeded at a density of 30,000 cells/cm², and cultured in growth medium supplemented with 10 mM sodium β-glycerophosphate (Sigma-Aldrich, USA) and 50 µg/mL ascorbic acid. After one week of culture, the substrates were washed with PBS and then the cells were lysed by 2% Triton X-100 for the analysis of total protein level and ALP activity. ALP activity was determined by QuantiChromTM Alkaline Phosphatase Assay Kit (BioAssay Systems, USA). Optical intensity was measured at 405 nm in a microplate reader. The amount of p-nitrophenol was quantified utilizing a standard curve obtained from known concentrations of p-nitrophenol. The Micro BCATM Protein Assay Kit (Thermo Scientific, USA) was used to determine the protein concentration with bovine serum albumin as the standard. ALP activity was expressed as

μM of *p*-nitrophenol formation per minute per microgram of total proteins.

Calcium deposition

Osteoblasts were seeded on each substrate at a density of 30,000 cells/cm², and cultured in the growth medium supplemented with 50 $\mu\text{g}/\text{mL}$ ascorbic acid and 10 mM sodium β -glycerophosphate. After 14 days of culture, each substrate was washed twice with deionized water, soaked in 1 mL of 2% nitric acid overnight with shaking to dissolve the calcium content on each surface. The calcium concentration in solution was then measured by using a QuantiChrom™ Calcium Assay Kit.³³

The deposited calcium was also investigated via alizarin red staining. After 14 days of culture, the medium was removed and osteoblasts on the substrates were washed with deionized water and stained with 2% alizarin red for 5 min. The substrates were then washed with deionized water and observed with microscope (Nikon, Japan). A negative control was obtained by immersion of pristine Ti in the medium with 50 $\mu\text{g}/\text{mL}$ ascorbic acid and 10 mM sodium β -glycerophosphate for 14 days without seeding osteoblasts.

Statistical analysis

At least three samples per time point for each experimental condition were used. The results were reported as mean \pm standard deviation and a one-way analysis of variance (ANOVA) was used to assess the data. Significant difference was accepted at $p < 0.05$.

Results and Discussion

Surface characterization of the pristine and treated Ti substrates

The XPS wide scan spectra and the surface elemental compositions of pristine Ti, Ti-PDOP, Ti-PDOP-curcumin10 and Ti-PDOP-curcumin20 substrates were shown in Fig. 1 and Table 1. Carbon was present in the wide scan spectrum of pristine Ti (Fig. 1a) because of inevitable hydrocarbon contamination. A small amount of N may be a result of the impurities in Ti. Deposition of polydopamine on Ti was indicated by an increase in the N and C contents (Fig. 1b and Table 1).¹⁶ The absence of Ti 2p peak for the Ti-PDOP substrate indicates that the substrate surface was totally covered with polydopamine (Fig. 1b). Upon attachment of curcumin on Ti-PDOP, the N content decreased (Figs. 1c, 1d and Table 1) due to the absence of N in curcumin (Fig. S1). The XPS C 1s and O 1s core-level spectra of Ti-PDOP, Ti-PDOP-curcumin10, and Ti-PDOP-curcumin20 were shown in Fig. S2.

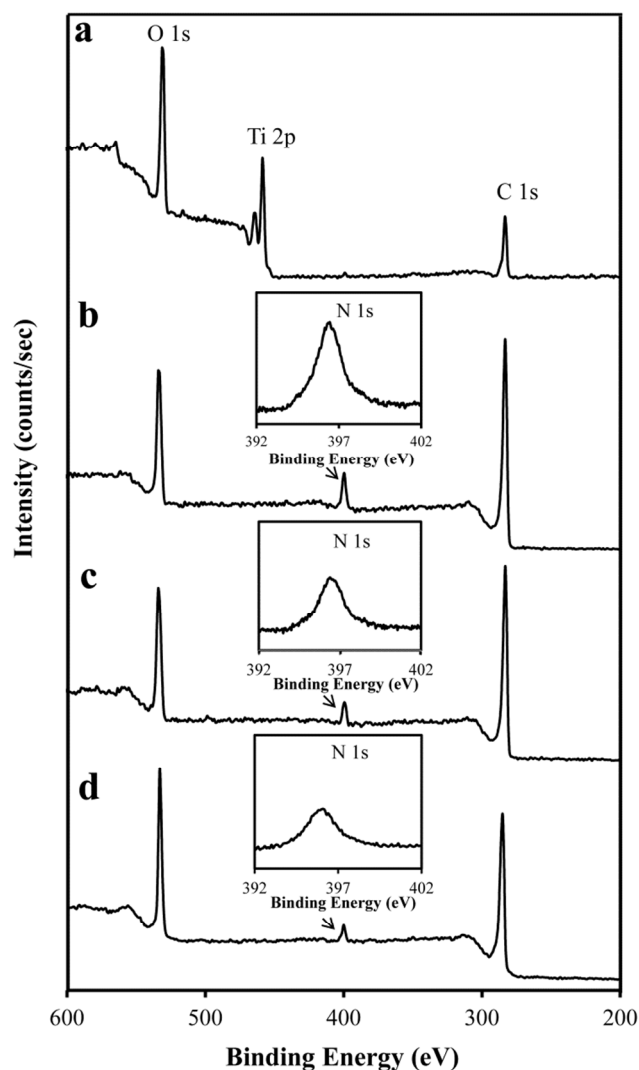


Fig. 1 XPS wide scan spectra of (a) Ti, (b) Ti-PDOP, (c) Ti-PDOP-curcumin10 and (d) Ti-PDOP-curcumin20. The insets show the N 1s core-level spectra of the Ti-PDOP, Ti-PDOP-curcumin10 and Ti-PDOP-curcumin20 substrates.

Table 1 Elemental compositions^a on the surfaces of the substrates as determined by XPS.

Substrate	Ti%	O%	N%	C%
Ti	12.8	44.1	1.0	42.1
Ti-PDOP	0.0	17.0	6.4	76.6
Ti-PDOP-curcumin10	0.0	19.1	4.3	76.6
Ti-PDOP-curcumin20	0.0	25.9	3.5	70.6

^aPercentages calculated based on the Ti, O, N, and C contents only.

Curcumin can generate fluorescence after illumination with excitation light at the wavelength of 425 nm, and the fluorescence intensity can be significantly enhanced after binding with HP- β -CD due to an effect of supramolecular host-

guest inclusion.^{33,34} Thus, the presence of curcumin on the Ti-PDOP-curcumin10 and Ti-PDOP-curcumin20 substrates can be directly observed under a fluorescence microscope after incubation of these substrates in a HP- β -CD solution. As shown in Figs. 2a and 2b, after treatment with HP- β -CD, no fluorescent signal was found on the pristine Ti and Ti-PDOP substrates, while positive green fluorescence signals were observed on the Ti-PDOP-curcumin10 and Ti-PDOP-curcumin20 substrates (Figs. 2c and 2d), indicating that curcumin was successfully immobilized on the substrates. As shown in Table 2, the surface density of loaded curcumin linearly increased from 0.23 ± 0.01 $\mu\text{g}/\text{cm}^2$ with the amount of curcumin in the loading solution increased from 0.37 μg (10 μM) to 0.74 μg (20 μM). The loading efficiency (defined as the percentage of curcumin in the loading solution that was loaded on the Ti-PDOP substrate) was about 60%. This loading efficiency of surface modification of Ti is much higher than that (10%) in the previous work in our group.¹⁷ The interaction between polydopamine and curcumin is still unknown. Polydopamine has amine groups⁴⁰ that bear positive charge in pH of 6-7.⁴¹ Curcumin was reported to bear a negative charge in pH of 7-9.⁴² The pH of the solution used in this study as well as the body fluid is around 7. In this situation, curcumin can form complexes with polydopamine due to the electrostatic interaction.⁴¹ Furthermore, the hydrogen bond between curcumin and the catechol groups in polydopamine⁴³ may further enhance its chemisorptions on polydopamine. However, further investigation is needed to demonstrate the phenomenon.

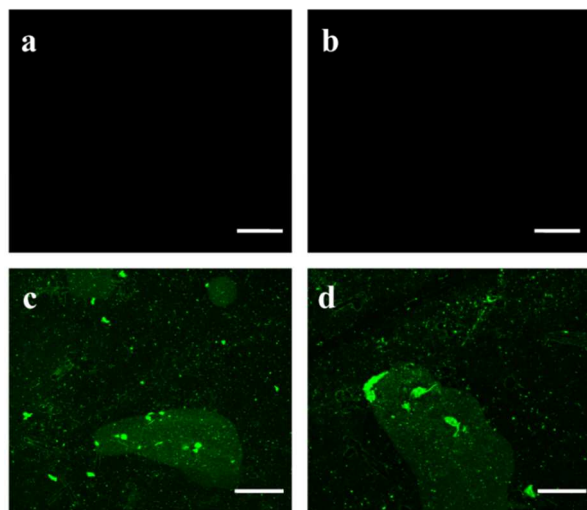


Fig. 2 CLSM images of (a) Ti, (b) Ti-PDOP, (c) Ti-PDOP-curcumin10 and (d) Ti-PDOP-curcumin20 substrates treated with HP- β -CD. Scale bar = 500 μm .

Table 2 Amount of loaded curcumin as determined by HPLC.

Substrate	Total amount in the loading solution (μg)	The amount in the combined washing solution (μg)	Surface density of loaded curcumin ($\mu\text{g}/\text{cm}^2$)
Ti-PDOP-Curcumin10	0.37	0.14 ± 0.01	0.23 ± 0.01
Ti-PDOP-Curcumin20	0.74	0.31 ± 0.04	0.43 ± 0.04

Curcumin release

Release tests were performed to analyze whether curcumin can be released from the substrates (Fig. 3). For the Ti-PDOP-curcumin10 and Ti-PDOP-curcumin20 substrates, about 90% of the initial loaded curcumin remained on the surface after incubation in PBS for 240 h. With further increase in the incubation time, no measurable release of curcumin was observed after 48 h. The remained curcumin on the surfaces was confirmed by CLSM images after treated with HP- β -CD (method mentioned above) in Fig. S3. This release result indicates that the loaded curcumin was strongly bound to the polydopamine layer, which is probably due to the mechanisms we discussed above (details see above). To investigate whether such level of curcumin release shows effects on cells, cells were treated with the growth medium supplemented with the same amount of curcumin, and the cytotoxicity was tested (details see below).

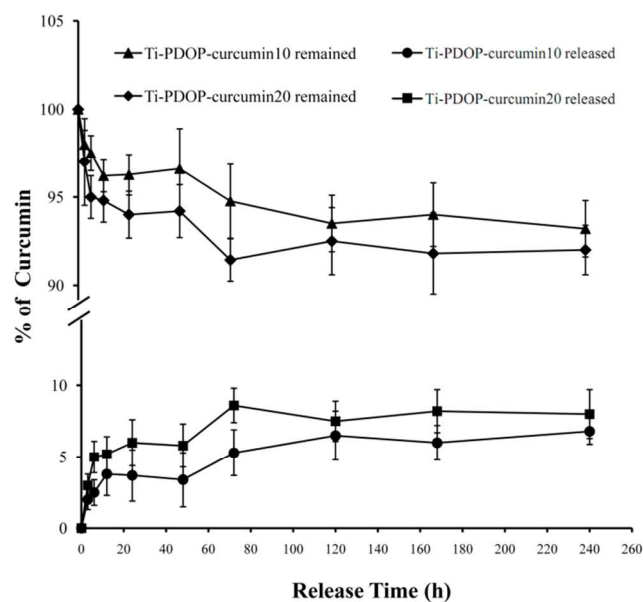


Fig. 3 Curcumin residence and release profiles for the Ti-PDOP-curcumin10 and Ti-PDOP-curcumin20 substrates ($n=3$) after incubation in PBS at room temperature over 240 h. The Ti-PDOP-curcumin10 and Ti-PDOP-curcumin20 remained curves indicate the relative amount of immobilized curcumin on the substrate after incubation for the predetermined periods, while the released curves indicate the cumulative release of the immobilized curcumin.

Fibroblast attachment, proliferation, and apoptosis

On the Ti-PDOP-curcumin10 and Ti-PDOP-curcumin20 substrates, fibroblast proliferation was reduced as compared to that on pristine Ti after 3 and 7 days of culture (Fig. 4a). Such

reduction in proliferation is not due to the reduction in the initial cell attachment since no significant difference in fibroblast attachment was observed on the pristine and curcumin-functionalized Ti substrates 6 h after cell seeding (Fig. S4). The MTT results also indicated reduced proliferation of fibroblasts on the curcumin-modified Ti substrates (Fig. 4b), which were consistent with the cell count results (Fig. 4a). In addition, we also investigated the effects of the released curcumin on fibroblasts on 48 h, and found that such level of curcumin release did not exhibit significant reduction in fibroblast proliferation (Fig. S5). Thus, the observed suppression in fibroblast proliferation (Fig. 4) is due to the loaded curcumin on the Ti substrates, not the released curcumin.

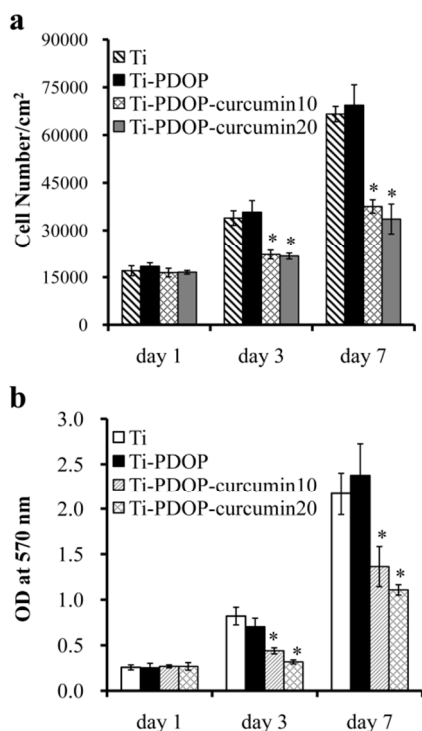


Fig. 4 (a) Fibroblast proliferation and (b) MTT assay results for the fibroblasts cultured on the Ti, Ti-PDOP, Ti-PDOP-curcumin10 and Ti-PDOP-curcumin20 substrates on day 1, 3, and 7 (n=3). * indicates significant difference ($p < 0.05$) compared with the Ti substrates.

Annexin V-FITC/PI staining assay is a commonly-used method to analyze cell apoptosis bioactivity.³⁷ After staining, apoptotic cells show green fluorescence, while little or no fluorescence can be observed for live cells. The fluorescence microscopy images show that fibroblasts on the Ti and Ti-PDOP substrates suffered minimal apoptosis, whereas significant apoptosis occurred on the Ti-PDOP-curcumin10 and Ti-PDOP-curcumin20 substrates (Fig. 5a). The quantitative results by flow cytometry analysis show that there was almost 4-fold increase in the percentages of apoptotic fibroblasts on the Ti-PDOP-curcumin10 and Ti-PDOP-curcumin20 substrates as compared with that on the pristine Ti substrate. Thus, the observed reductions in fibroblast proliferation on Ti-PDOP-

curcumin10 and Ti-PDOP-curcumin20 (Fig. 4a) properly result from fibroblast apoptosis induced by modified curcumin. Previous *in vitro* study has indicated that the concentration of curcumin to induce fibroblast apoptosis is about 5–25 μM (2–10 $\mu\text{g/mL}$),²² but the relevant data for immobilized curcumin are not available. Our results show that with a surface density of loaded curcumin of $0.23 \pm 0.01 \mu\text{g/cm}^2$, a significant fibroblast apoptosis and suppression in fibroblast proliferation was attained.

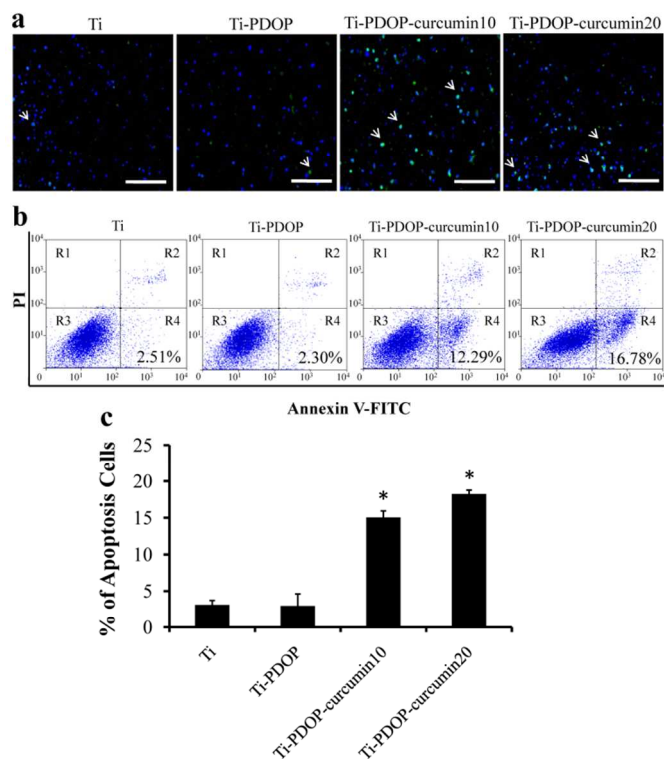


Fig. 5 Apoptosis of fibroblasts on Ti, Ti-PDOP, Ti-PDOP-curcumin10 and Ti-PDOP-curcumin20 substrates 48 h after cell seeding: (a) Fluorescence microscopy images of fibroblasts on the pristine and functionalized Ti substrates. All the nuclei exhibited blue fluorescence, and the appearance of green fluorescence (as marked with white arrows) indicated apoptosis. Scale bar = 500 μm . (b) Flow cytometry analysis of the fibroblasts after staining with Annexin V-FITC/PI. In each section, the left upper quadrant (R1) and the right upper quadrant (R2) represented necrotic cells and dead cells, respectively; the left lower quadrant (R3) and the right lower quadrant (R4) represented live cells and apoptosis cells (marked with percentage), respectively. (c) Percentages of apoptotic cells on the pristine and functionalized Ti substrates determined by flow cytometry analysis (n=3). The results of positive control were shown in Fig. S6. * indicates $p < 0.05$ compared with the Ti substrates.

The mechanism by which curcumin induces apoptosis in fibroblasts is still unclear. Soluble curcumin may induce cell apoptosis via the activation of caspases by either the upregulation in the expression of the members of the TNF (tumor necrosis factor) receptor family such as TRAIL-R1 (TNF-related apoptosis inducing ligand-receptor 1) or TRAIL-R2,^{28,44} or the induction of cytochrome c to interact with apoptotic protease activating factor-1 (Apaf-1).^{45–47} In addition, soluble curcumin also has the ability to induce apoptosis through oxidative stress signals. Scharstul et al. report that for curcumin-treated fibroblasts, the expression of heme

oxygenase-1 molecule (a main endogenous antioxidant) was downregulated, and the reactive oxygen species (which act to induce apoptosis) was increased.²² In contrast, curcumin is found to be a potent scavenger of reactive oxygen species; thus, it is difficult to establish a mechanistic basis by this mechanism for apoptosis induced by curcumin due to the complexity of redox regulation by curcumin.⁴⁸ Nevertheless, according to the best of our knowledge, the mechanism by which the immobilized curcumin can induce fibroblast apoptosis has not been investigated, and further studies are required.

Collagen assay and genes expression

Fig. 6a qualitatively shows that the amounts of collagen produced by fibroblasts on the Ti-PDOP-curcumin10 and Ti-PDOP-curcumin20 substrates were significant reduced comparing to that on pristine Ti on days 7 and 14. Quantitative results show that the amounts of collagen on the Ti-PDOP-curcumin10 and Ti-PDOP-curcumin20 substrates were ~60% lower than that on the pristine Ti substrate after 7 and 14 days of culture ($p < 0.05$) (Fig. 6b). Collagen type I is the main component in fibrous tissue⁴⁹ and the deposition of collagen by fibroblasts is responsible for the development of fibrous encapsulation.^{50,51} Therefore, the collagen assay results in this study indicate that the curcumin-modified surfaces may be a promising solution to combat fibrous encapsulation.

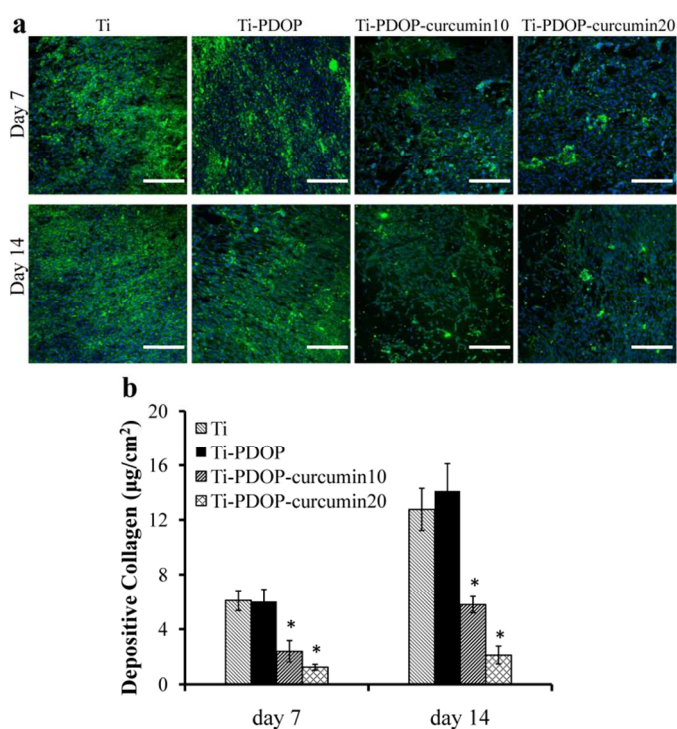


Fig. 6 Collagen generated by fibroblasts on Ti, Ti-PDOP, Ti-PDOP-curcumin10 and Ti-PDOP-curcumin20. (a) CLSM images of stained collagen (green) on the different substrates on days 7 and 14. Scale bar = 500 μm . (b) Quantification of collagen type I generated by fibroblasts on the different substrates on days 7 and 14 ($n=3$). * indicates $p < 0.05$ compared with the Ti substrates.

As fibroblasts are the principle cells for collagen synthesis, the reason for the reductions of collagen deposition on

curcumin-modified Ti may be the effect of fibroblast apoptosis caused by loaded curcumin. Interestingly, collagen deposition on Ti-PDOP-curcumin20 was significantly lower than that on Ti-PDOP-curcumin10 ($p < 0.05$) (Fig. 6b), but the degree of fibroblast apoptosis was not significantly different on these substrates (Fig. 5c). This indicates that besides fibroblast apoptosis, there may be other effects responsible for the immobilized curcumin to reduce collagen generation by fibroblasts, which is worth further investigation.

In addition to the collagen assay, the effects of the loaded curcumin on fibroblasts at genetic level, i.e. the gene expressions of fibrotic markers such as *Acta2*, *Colla1*, and *Fnl*, were investigated (Fig. 7). The gene expressions of fibrotic markers by fibroblasts on the curcumin-modified substrates were significantly reduced compared to that on pristine Ti on day 7 (Fig. 7a) and day 14 (Fig. 7b). The gene *Acta2* is a marker of myofibroblasts,⁵² a type of cells that are differentiated from fibroblasts and characterized by synthesis of collagen type I.⁵³ The reduced expression of *Acta2* in our study indicates that the immobilized curcumin can prevent the differentiation of fibroblasts to myofibroblasts, and this effect contributes to the reduction in collagen production as observed above. The gene *Colla1* regulates the expression of collagen type I,⁵⁴ and the downregulation of its expression suggests the suppression in the ability of collagen synthesis by fibroblasts. *Fnl* regulates the expression of fibronectin, which is an enhancement factor for fibroblast proliferation,⁵⁵ and the observed reduction in the expression of *Fnl* by fibroblasts (Figs. 7a and 7b) indicates that the immobilized curcumin exhibited a negative effect on fibroblast proliferation (Fig. 4). From these gene expression results, it is shown that the observed reduction in collagen synthesis by the fibroblasts on the curcumin-modified substrates may result from the effects of curcumin on impeding the differentiation of fibroblasts to myofibroblasts, and reducing the proliferation and collagen synthesis ability of fibroblasts.

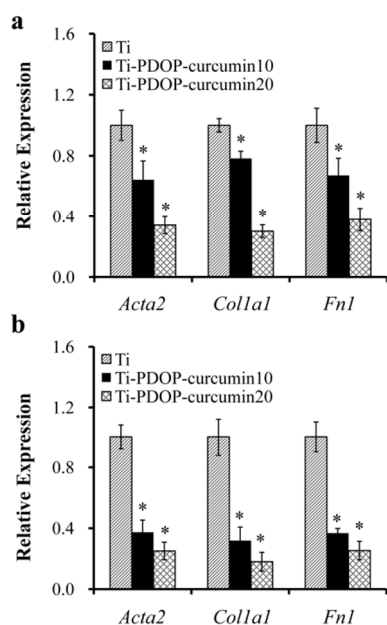


Fig. 7 Relative gene expressions by fibroblasts on Ti, Ti-PDOP-curcumin10 and Ti-PDOP-curcumin20 after (a) 7 and (b) 14 days of culture (n=3). * indicates $p < 0.05$ compared with the Ti substrates.

The mechanism by which curcumin can influence fibroblast differentiation remains unknown. It has been reported that curcumin can inhibit the nuclear factor kappa-light-chain-enhancer of activated B cells (NF- κ B)-dependent pathway, resulting in the inhibition of fibroblast differentiation into myofibroblasts.²⁷ Curcumin was also reported to activate peroxisome proliferator-activated receptor gamma (PPAR- γ), a nuclear receptor that can reduce the proliferation of fibroblasts.⁵⁴ However, it was unclear whether this activation is due to the binding of curcumin to PPAR- γ ,⁵⁶ or a result of other possible indirect effects.⁵⁴ Li et al. has proved that curcumin reduces the expression of *Acta2* via extracellular regulated protein kinases (ERK)-dependent pathway, which is the key pathway of fibroblast differentiation.⁵⁷

Osteoblast attachment, proliferation, apoptosis, differentiation and calcium deposition

Osteoblasts are the major cellular component of bone and the principle cells for osteogenesis and osseointegration.⁵⁸ Thus, it is necessary to investigate whether the immobilized curcumin exhibits adverse effects on osteoblast functions. As shown in Fig. 8, the loaded curcumin did not significantly reduce osteoblast attachment (Fig. 8a) and proliferation (Figs. 8b and 8c). Since a minor portion of the immobilized curcumin will release into the cell culture medium (see above), the effect of the released curcumin on osteoblast functions was also investigated (Fig S7 in the Supporting Information). As shown in Fig S7, the released curcumin did not adversely affect the proliferation of osteoblasts. The apoptosis results (Fig. S8) also indicate that the immobilized curcumin did not induce significant apoptosis in osteoblasts.

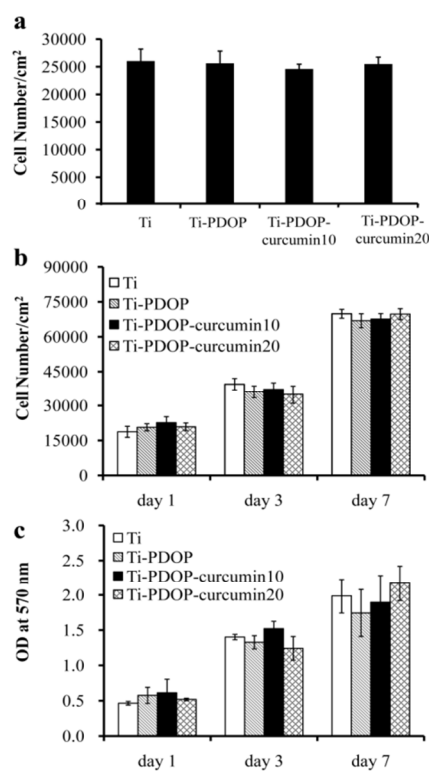


Fig. 8 (a) The number of adherent osteoblasts on the Ti, Ti-PDOP, Ti-PDOP-curcumin10, and Ti-PDOP-curcumin20 substrates 6 h after cell seeding. (b) Cell numbers and (c) MTT assay results of osteoblasts on day 1, 3, and 7 (n=3).

The effect of immobilized curcumin on ALP activity, an early marker for the osteoblast differentiation, was analyzed after one week on the different substrates. As shown in Fig. 9, the loaded curcumin did not significantly reduce osteoblast ALP activity. The results indicate that the immobilized curcumin had no adverse effect on the ALP activity of osteoblasts.

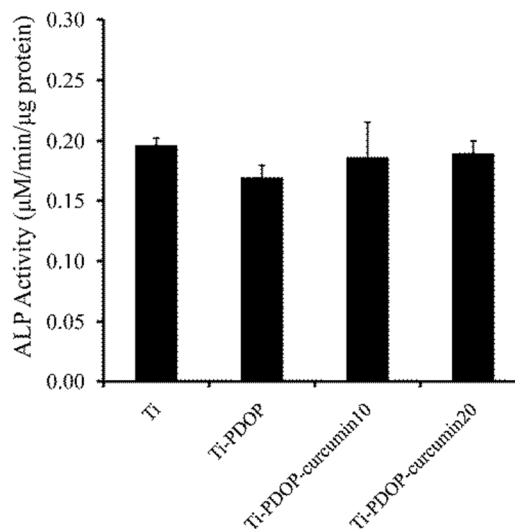


Fig. 9 ALP activity of osteoblasts cultured on the Ti, Ti-PDOP, Ti-PDOP-curcumin10 and Ti-PDOP-curcumin20 substrates. ALP, alkaline phosphatase.

Calcium deposition by osteoblasts is qualitatively evaluated by alizarin red staining. The results of alizarin red staining show that the level of calcium depositions by osteoblasts on the curcumin-functionalized substrates was similar to that on the pristine Ti substrate over 14 days (Figs. 10a-d), and the quantitative calcium deposition results obtained with the curcumin-modified substrates were not significant different from that with Ti (Fig. 10f). These results indicate that the immobilized curcumin had no adverse effect on the mineralization of osteoblasts.

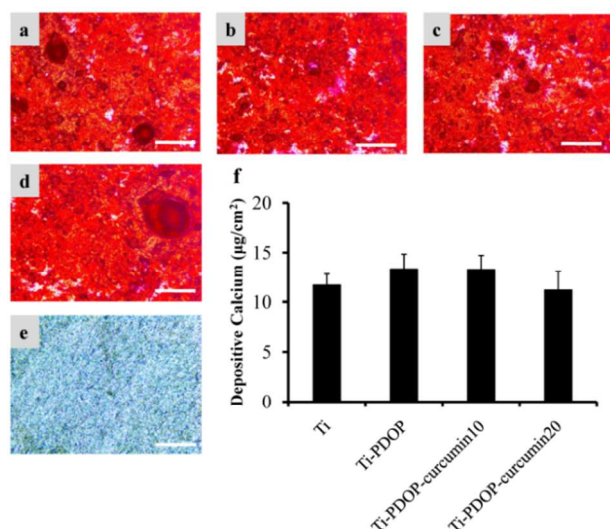


Fig. 10 Alizarin red staining of the deposited calcium by osteoblasts on (a) Ti, (b) Ti-PDOP, (c) Ti-PDOP-curcumin10 and (d) Ti-PDOP-curcumin20. (e) Alizarin red staining on Ti without seeded cells after immersion in medium for 14 days. Scale bar = 500 µm. (f) Quantification of the deposited calcium by osteoblasts on the different substrates (n=3).

Curcumin was reported to inhibit the proliferation and mineralization of osteoblasts at a concentration ranging from 5 µM (1.8 µg/mL) to 10 µM (3.7 µg/mL)⁵⁹, but the relevant data for immobilized curcumin are not available. However, the mechanisms by which curcumin affect the activities of osteoblasts are still unknown. From the results observed in this study that fibroblasts and osteoblasts exhibit different responses towards the same curcumin-modified surface (Ti-PDOP-curcumin10 and Ti-PDOP-curcumin20), it can be proposed that the immobilized curcumin may influence the functions of fibroblasts and osteoblasts via different pathways. Thus, further investigation is needed to demonstrate the phenomenon. These findings may be highly desirable for orthopedic applications.

Conclusions

Curcumin was loaded on Ti substrates by using polydopamine as an anchor, and most of the loaded curcumin remained on the substrate even after 7 days of immersion in PBS. The fibroblast functions were significantly reduced on curcumin-modified substrates possibly due to an increase in fibroblast apoptosis and a reduction in the expression of relative genes induced by the surface curcumin. In contrast, no significant reduction in

osteoblast functions was observed on the curcumin-modified substrates. Thus, these *in vitro* results highlight the concept of surface-loaded curcumin on implants for reducing fibrous encapsulation, which may offer promising strategies in orthopedic applications to reduce implant loosening.

Acknowledgements

This work was financially supported by the National Medical Research Council of Singapore Grant NMRC/1258/2010.

Notes and references

^aDepartment of Orthopedic Surgery, National University of Singapore, 1E Kent Ridge Road, NUHS Tower Block Level 11, 119228, Singapore.

^bDepartment of Joint and Trauma Surgery, the Third Affiliated Hospital of Sun Yat-sen University, Guangzhou, 510000, China.

^cDepartment of Mechanical Engineering, National University of Singapore, Kent Ridge, 117576, Singapore. E-mail: jakeho1986@gmail.com; doswangw@nus.edu.sg; Fax: +65-67744082; Tel: +65-67795555

† Footnotes should appear here. These might include comments relevant to but not central to the matter under discussion, limited experimental and spectral data, and crystallographic data.

Electronic Supplementary Information (ESI) available: [details of any supplementary information available should be included here]. See DOI: 10.1039/b000000x/

- I. D. Learmonth, C. Young and C. Rorabeck, *Lancet*, 2007, **370**, 1508-1519.
- V. Goldberg, *Instr. Course Lect.*, 2001, **50**, 357.
- J. Baas, T. Jakobsen, B. Elmengaard, J. E. Bechtold and K. Soballe, *J. Biomed. Mater. Res., Part A.*, 2010, **100A**, 188-194.
- P. Kinov, A. Leithner, R. Radl, K. Bodo, G. A. Khoschsorur, K. Schauenstein and R. Windhager, *J. Orthop. Res.*, 2006, **24**, 55-62.
- J. M. Anderson, A. Rodriguez and D. T. Chang, *Semin. Immunol.*, 2008, **20**, 86-100.
- A. Mavrogenis, R. Dimitriou, J. Parvizi and G. Babis, *J. Musculoskelet. Neuronal. Interact.*, 2009, **9**, 61-71.
- Y. T. Konttinen, D. Zhao, A. Beklen, G. Ma, M. Takagi, M. Kivelä-Rajamäki, N. Ashammakhi and S. Santavirta, *Clin. Orthop. Relat. Res.*, 2005, **430**, 28-38.
- H. M. Van Der Vis, P. Aspenberg, R. K. Marti, W. Tigchelaar and C. J. Van Noorden, *Clin. Orthop. Relat. Res.*, 1998, **350**, 201-208.
- S. Schultze-Mosgau, M. B. Blatz, F. Wehrhan, K. A. Schlegel, M. Thorwart and S. Holst, *QuintessenceInt.*, 2005, 36.
- A. Sabokbar, I. Itonaga, S. Sun, O. Kudo and N. Athanasou, *J. Orthop. Res.*, 2005, **23**, 511-519.
- X. Pan, X. Mao, T. Cheng, X. Peng, X. Zhang, Z. Liu, Q. Wang and Y. Chen, *J. Surg. Res.*, 2012, **176**, 484-489.

- 12 A. B. Novaes Jr, S. Souza, R. Barros, K. Pereira, G. Iezzi and A. Piattelli, *Braz. Dent. J.*, 2010, **21**, 471-481.
- 13 A. S. Brack, M. J. Conboy, S. Roy, M. Lee, C. J. Kuo, C. Keller and T. A. Rando, *Science*, 2007, **317**, 807-810.
- 14 M. Ponnusamy, L. Ma, R. Gong, M. Pang, Y. E. Chin and S. Zhuang, *Am. J. Physiol. Renal. Physiol.*, 2011, **300**, F62.
- 15 J. Aubin, F. Liu, L. Malaval and A. Gupta, *Bone*, 1995, **17**, S77-S83.
- 16 H. C. Tan, C. K. Poh, Y. Cai and W. Wang, *J. Orthop. Res.*, 2013, **31**, 983-990.
- 17 X. Hu, K. G. Neoh, Z. Shi, E. T. Kang and W. Wang, *Tissue Eng., Part A*, 2013, **19**, 1919-1930.
- 18 J. Y. Lee, Y. S. Choi, S. J. Lee, C. P. Chung and Y. J. Park, *Curr. Pharm. Des.*, 2011, **17**, 2663-2676.
- 19 V. Patel, N. M. McLeod, S. N. Rogers and P. A. Brennan, *Br. J. Oral. Maxil. Surg.*, 2011, **49**, 251-257.
- 20 Y. Yu, X. Zhang and L. Qiu, *Biomaterials*, 2014, **35**, 3467-3479.
- 21 R. K. Maheshwari, A. K. Singh, J. Gaddipati and R. C. Srimal, *Life Sci.*, 2006, **78**, 2081-2087.
- 22 A. Scharstuhl, H. Mutsaers, S. Pennings, W. Szarek, F. Russel and F. Wagener, *J. Cell Mol. Med.*, 2009, **13**, 712-725.
- 23 H. Hatcher, R. Planalp, J. Cho, F. M. Torti and S. V. Torti, *Cell Mol. Life Sci.*, 2008, **65**, 1631-1652.
- 24 Q. Y. Yao, B. L. Xu, J. Y. Wang, H. C. Liu, S. C. Zhang and C. T. Tu, *BMC Complem. Altern. M.*, 2012, **12**, 156.
- 25 D. Punithavathi, N. Venkatesan and M. Babu, *Brit. J. Pharmacol.*, 2000, **131**, 169-172.
- 26 J. Lipecka, C. Norez, N. Bensalem, M. Baudouin-Legros, G. Planelles, F. Becq, A. Edelman and N. Davezac, *J. Pharmacol. Exp. Ther.*, 2006, **317**, 500-505.
- 27 J. Gaedeke, N. A. Noble and W. A. Border, *Kidney Int.*, 2004, **66**, 112-120.
- 28 D. Zhang, C. Huang, C. Yang, R. J. Liu, J. Wang, J. Niu and D. Bromme, *Respi. Res.*, 2011, **12**, 154.
- 29 M. R. Smith, S. R. Gangireddy, V. R. Narala, C. M. Hogaboam, T. J. Standiford, P. J. Christensen, A. K. Kondapi and R. C. Reddy, *Am. J. Physiol. Lung Cell Mol. Physiol.*, 2010, **298**, L616.
- 30 A. L. Cheng, C. H. Hsu, J. K. Lin, M. M. Hsu, Y. F. Ho, T. S. Shen, J. Y. Ko, J. T. Lin, B. R. Lin, M. S. Wu, H. S. Yu, S. H. Jee, G. S. Chen, T. M. Chen, C. A. Chen, M. K. Lai, Y. S. Pu, M. H. Pan, Y. J. Wang, C. C. Tsai and C. Y. Hsieh, *Anticancer Res.*, 2001, **21**, 2895-2900.
- 31 T. A. Barber, S. L. Golledge, D. G. Castner, and K. E. Healy, *J. Biomed. Mater. Res. A*, 2003, **64**, 38-47.
- 32 C. K. Poh, Z. Shi, X. W. Tan, Z. C. Liang, X. M. Foo, H. C. Tan, K. G. Neoh and W. Wang, *J. Orthop. Res.*, 2011, **29**, 1424-1430.
- 33 B. Tang, L. Ma, H. Y. Wang and G. Y. Zhang, *J. Agric. Food Chem.*, 2002, **50**, 1355-1361.
- 34 K. N. Baglolle, P. G. Boland and B. D. Wagner, *J. Photoch. Photobio. A*, 2005, **173**, 230-237.
- 35 G. K. Jayaprakasha, L. Jagan Mohan Rao and K. K. Sakariah, *J. Agric. Food Chem.*, 2002, **50**, 3668-3672.
- 36 Z. Shi, K. G. Neoh, S. Zhong, L. Yung, E. Kang and W. Wang, *J. Biomed. Mater. Res. A*, 2006, **76**, 826-834.
- 37 J. Pan, Q. Chang, X. Wang, Y. Son, Z. Zhang, G. Chen, J. Luo, Y. Bi, F. Chen and X. Shi, *Chem. Res. Toxicol.*, 2010, **23**, 568-577.
- 38 J. E. Kolodsick, G. B. Toews, C. Jakubzick, C. Hogaboam, T. A. Moore, A. McKenzie, C. A. Wilke, C. J. Chrisman and B. B. Moore, *J. Immunol.*, 2004, **172**, 4068-4076.
- 39 S. Dinescu, B. Galateanu, M. Albu, A. Cimpean, A. Dinischiotu and M. Costache, *Int. J. Mol. Sci.*, 2013, **14**, 1870-1889.
- 40 H. Lee, S. M. Dellatore, W. M. Miller, and P. B. Messersmith, *Science*, 2007, **318**, 426-430.
- 41 B. H. Choi, Y. S. Choi, D. S. Hwang and H. J. Cha, *Tissue Eng., Part C*, 2012, **18**, 71-79.
- 42 Z. Wang, M. H. Leung, T. W. Kee and D. S. English, *Langmuir*, 2010, **26**, 5520-5526.
- 43 P. Sanphui, N. R. Goud, U. R. Khandavilli and A. Nangia, *Cryst. Growth Des.*, 2011, **11**, 4135-4145.
- 44 J. Ryu, S. H. Ku, H. Lee and C. B. Park, *Adv. Funct. Mater.* 2010, **20**, 2132-2139.
- 45 F. Song, L. Zhang, H. X. Yu, R. R. Lu, J. D. Bao, C. Tan and Z. Sun, *Food Chem.*, 2012, **132**, 43-50.
- 46 R. J. Anto, A. Mukhopadhyay, K. Denning and B. B. Aggarwal, *Carcinogenesis*, 2002, **23**, 143-150.
- 47 D. Morin, S. Barthelemy, R. Zini, S. Labidalle and J. P. Tillement, *FEBS letters*, 2001, **495**, 131-136.
- 48 S. K. Borra, P. Gurumurthy and J. Mahendra, *J. Med. Plants Res.*, 2013, **7**, 2680-2690.
- 49 M. Ivarsson, A. McWhirter, T. K. Borg and K. Rubin, *Matrix Biol.*, 1998, **16**, 409-425.
- 50 J. M. Anderson, *Annu. Rev. Mater. Res.*, 2001, **31**, 81-110.
- 51 P. H. Zepelin, A. Larena-Avellaneda and K. Schmidt, *Plast. Reconstr. Surg.*, 2010, **126**, 266-274.
- 52 B. Hinz, G. Gabbiani and C. Chaponnier, *J. Cell Biol.*, 2002, **157**, 657-663.
- 53 G. Serini, M. L. Bochaton-Piallat, P. Ropraz, A. Geinoz, L. Borsi, L. Zardi and G. Gabbiani, *J. Cell Biol.*, 1998, **142**, 873-881.
- 54 V. R. Narala, M. R. Smith, R. K. Adapala, R. Ranga, K. Panati, B. B. Moore, T. Leff, V. D. Reddy, A. K. Kondapi and R. C. Reddy, *Gene Ther. Mol. Biol.*, 2009, **13**, 20.
- 55 R. A. Clark, J. Q. An, D. Greiling, A. Khan and J. E. Schwarzbauer, *J. Invest. Dermatol.*, 2003, **121**, 695-705.
- 56 A. Chen and J. Xu, *Am. J. Physiol. Gastrointest. Liver Physiol.*, 2005, **288**, G447-G456.
- 57 R. Li, Y. Wang, Y. Liu, Q. Chen, W. Fu, H. Wang, H. Cai, W. Peng and X. Zhang, *Plos One*, 2013, **8**, e58848.
- 58 G. Sajithlal, P. Chithra and G. Chandrakasan, *Biochem. Pharmacol.*, 1998, **56**, 1607-1614.
- 59 M. Notoya, H. Nishimura, J. T. Woo, K. Nagai, Y. Ishihara and H. Hagiwara, *Eur. J. Pharmacol.*, 2006, **534**, 55-62.